JOURNAL OF MATERIALS SCIENCE 40 (2005) 1655– 1659

Microhardness indentation size effect studies in $60B_2O_3$-(40-x)PbO-$x$$MCl_2$ and $50B_2O_3$-(50-x)PbO-$x$$MCl_2$ (M = Pb, Cd) glasses

S. SEBASTIAN
School of Pure and Applied Physics, Mahatma Gandhi University, Priyadarshini Hills P.O., Kottayam 686 560, India

M. A. KHADAR*
Department of Physics, University of Kerala, Kariavattom P.O., Thiruvananthapuram 695 581, India
E-mail: mabdulkhadar@rediffmail.com

The microhardness of glasses of the system $60B_2O_3$-(40-x)PbO-$x$$MCl_2$ and $50B_2O_3$-(50-x)PbO-$x$$MCl_2$ (M = Cd, Pb) was investigated for 20 different compositions over a wide range of applied loads. The microhardness number was found to increase rapidly at lower values of the load, then to increase at a slower rate and finally it attained a constant value above 200 g load. The load dependence of the apparent hardness in the low load region is discussed. The indentation size effect (ISE) on the microhardness is discussed and the load independent true microhardness values are evaluated. The dependence of true microhardness value with increase in mole percentage of $PbCl_2$ or $CdCl_2$ is discussed based on the expansion of the borate matrix.

1. Introduction

Microhardness is an important parameter often used to define the mechanical properties of a material on a microscopic scale [1]. In a diamond pyramid microhardness tester, a diamond indenter is impressed on a surface at a known load for a known period of time. The area of indentation remaining after removal of the indenter is calculated from the width of the impression of the indenter. The applied load divided by area of the indentation is defined as the hardness (H). Accurate measurements of the hardness of brittle materials have been difficult due to the dependence of hardness on load [2]. This presents a problem to investigators because in the load dependent region making comparison between hardness of materials is difficult. The shape of the diamond indenter in microhardness testing can be square pyramid (Vickers) or elongated pyramid (Knoop). Vickers (square pyramid) indentation method is best suitable for hardness measurements in glasses and other brittle materials, because the contact pressure for a pyramid indenters are independent of the indent size and maintains geometry of the indentation pattern even after the onset of cracking.

The indenter gives geometrically similar indentation, so that the measured hardness must be independent of the applied load [2]. But it is experimentally well established that apparent hardness measured in a low load range decreases [3–5] or increases [6–8] with increase in applied load. According to Gong and Li [9], the former is called indentation size effect (ISE) and the latter is called reverse indentation size effect (RISE). ISE is traditionally described on the basis of Mayer's law [10].

$$P = Ad^{\mathrm{n}} \tag{1}$$

where P is the indentation test load and d is the resulting indentation size. A and n are descriptive parameters derived from the curve fitting of the experimental results. The value of n is expected to be 2 in the absence of ISE [5]. Although the Mayer law has been well proved to be suitable for representing the experimental data, neither an explanation of the physical meaning of the power exponent nor the cause of the indentation size effect has been satisfactorily achieved [5]. The load dependence of the hardness was studied on the basis of variety of phenomena, and several empirical equations were proposed for representing experimental data [5, 11–13].

Recently Gong and Li [9] based on energy balance consideration originally proposed by Frohlich *et al.* [14] derived a semi empirical equation to estimate the true hardness of the test specimen independent of the indenter geometry as well as indentation size. The validity of the semi empirical equation was examined using previously published experimental data, in which apparent hardness increases with decrease in load. Gong and Li [9] proposed that, the same equation can be used to

---

*Author to whom all correspondence should be addressed.

evaluate the true hardness when the apparent hardness value increases with increase in indentation size known as reverse indentation size effect (RISE). The reports on RISE in glasses are very limited. To examine ISE or RISE critically it is necessary to evaluate an extensive set of experimental microhardness measurements on one material or related materials. Glasses can be used to examine ISE critically because glasses have certain advantages over their crystalline counter part. Glasses are isotropic and avoid the problems associated with the grain boundaries in poly crystalline materials. Also there is a possibility of continuously varying the glass composition.

The purpose of the present work is to examine the RISE based on the energy balance considerations proposed by Gong and Li [9] on 4 set of glass samples ($60B_2O_3$-(40-x)PbO-xMCl$_2$ and $50B_2O_3$-(50-x) PbO-xMCl$_2$ (M = Cd, Pb) for different compositions. The load independent microhardness values of these glass samples are calculated using the empirical relation given by Gong and Li [9]. The calculated true hardness values were compared with experimentally determined microhardness values. The variations of true hardness values with addition of $PbCl_2$ or $CdCl_2$ in the glass systems are discussed.

2. Experimental

$60B_2O_3$-(40-x)PbO-xMCl$_2$ and $50B_2O_3$-(50-x)PbO-xMCl$_2$ (M = Cd,Pb) (x = 10, 12.5, 15, 17.5, 20) glasses of different compositions (Tables I and II) were prepared from appropriate amounts of analar grade H_3BO_3, PbO, and $CdCl_2$ or $PbCl_2$. Calculated quantities of the chemicals were mixed thoroughly in an agate mortar and heated in an electric furnace for 1 h at 500°C in a porcelain crucible. This ensured the complete decomposition of H_3BO_3. During the preparation of glasses containing $PbCl_2$ or $CdCl_2$ considerable amount of vapour loss (Chlorine) occurs during the melting process. To minimize such a loss the closed crucible was immediately transferred in to another furnace kept at 850 to 950°C depending upon composition. The melting process was continued for 15 min. The melt was then poured in to a brass mould and pressed by another, to quench the melt and to obtain glass discs of diameter 2 cm and thickness 1 cm. The samples were then annealed in a furnace preheated to 300°C for 3 h and then allowed to cool to room temperature. The samples were then polished using fine grade emery papers.

The micro hardness of the glass samples was measured by using Vickers indentation method. A hardness tester (Leitz miniload L) fitted with a diamond pyramidal indenter, attached to an incident light microscope was used for the study. The Vickers diamond indenter was applied perpendicular to the glass samples at different sites having no surface defects. The load P was varied from 5 to 500 g and the time of indentation was kept constant at 30 s for all measurements. The distance between any two indentations was kept more than five times the diagonal length of the

TABLE I Sample code, glass composition, best fit parameters in Equation 3, True hardness, and measured hardness for a load 200 gm of samples $60B_2O_3$-(40-x) PbO-xPbCl$_2$ and $50B_2O_3$-(50-x) PbO-xPbCl$_2$ of different composition

		Best fit parameters in Equation 3			Microhardness values (GPa)	
Sample code	Glass composition	a_0 (J/m)	$a_1 \times 10^3$ (J/m^2)	$a_2 \times 10^6$ (J/m^3)	True microhardness (H_T)	Measured hardness at 200 g load (H_v)
BPP1	$60B_2O_3$-30PbO-10PbCl$_2$	−0.421	3.06	2054.67	3.81	3.78
BPP2	$60B_2O_3$-27.5PbO-12.5PbCl$_2$	−0.302	9.64	2074.46	3.85	3.78
BPP3	$60B_2O_3$-25PbO-15PbCl$_2$	−0.641	31.17	2047.15	3.80	4.47
BPP4	$60B_2O_3$-22.5PbO- 17.5PbCl$_2$	−0.615	27.61	1954.96	3.61	4.01
BPP5	$60B_2O_3$-20PbO-20PbCl$_2$	−0.752	32.09	1893.95	3.51	4.04
BPP6	$50B_2O_3$-40PbO-10PbCl$_2$	−0.688	16.88	2096.31	3.88	3.92
BPP7	$50B_2O_3$-37.5PbO-12.5PbCl$_2$	−1.183	43.18	2164.92	4.01	4.47
BPP8	$50B_2O_3$-35PbO-15PbCl$_2$	−0.760	26.413	2043.26	3.84	4.04
BPP9	$50B_2O_3$-32.5PbO-17.5PbCl$_2$	−0.813	28.375	1941.31	3.6	3.91
BPP10	$50B_2O_3$-30PbO-20PbCl$_2$	−1.223	46.316	1960.48	3.52	4.04

TABLE II Sample code, glass composition, best fit parameters in Equation 3, True hardness, and measured hardness for a load 200 gm of samples $60B_2O_3$-(40-x) PbO-xPbCl$_2$ and $50B_2O_3$-(50-x) PbO-xPbCl$_2$ of different composition

		Best fit parameters in Equation 3			Microhardness values (GPa)	
Sample code	Glass composition	a_0 (J/m)	$a_1 \times 10^3$ (J/m^2)	$a_2 \times 10^6$ (J/m^3)	True microhardness (H_T)	Measured hardness at 200 g load (H_v)
BPC1	$60B_2O_3$-30PbO-10cDCl$_2$	−0.504	16.75	2436.32	4.52	4.81
BPC2	$60B_2O_3$-27.5PbO-12.5CdCl$_2$	−0.527	19.33	2269.33	4.21	4.64
BPC3	$60B_2O_3$-25PbO-15CdCl$_2$	−0.598	29.77	1852.02	3.43	4.04
BPC4	$60B_2O_3$-22.5PbO- 17.5CdCl$_2$	−0.601	34.86	1839.84	3.41	4.32
BPC5	$60B_2O_3$-20PbO-20CdCl$_2$	−0.476	32.97	1731.17	3.21	4.18
BPC6	$50B_2O_3$-40PbO-10CdCl$_2$	−0.543	19.91	2214.64	4.11	4.14
BPC7	$50B_2O_3$-37.5PbO-12.5CdCl$_2$	−0.576	28.25	2131.8	3.95	4.47
BPC8	$50B_2O_3$-35PbO-15CdCl$_2$	−0.577	29.84	2041.57	3.78	4.47
BPC9	$50B_2O_3$-32.5PbO-17.5CdCl$_2$	−0.435	19.73	1914.32	3.55	4.47
BPC10	$50B_2O_3$-30PbO-20CdCl$_2$	−0.657	38.59	1719.44	3.18	4.64

indentation, to avoid mutual influence of the indentations. For each load, ten trials of indentation were carried out and the average value of the diagonal length of indentation marks was determined. The indentations were carried out at room temperature. The diagonal length measurement was made on selected impressions having perfect square shape.

The hardness number H is defined as the ratio of applied load (P) to the contact area (A), between indenter and the sample i.e.

$$H = P/A$$

In the case of square based Vickers microhardness tester, microhardness number H_v were calculated using the relation

$$H_v = 1.8544P/d^2\,(\mathrm{K_g/mm^2}) \qquad (2)$$

where P is the applied load in K_g and d is the diagonal length of the indentation in mm.

Gong and Li [9] modified Equation 2 by considering the energy balance consideration and proposed an empirical equation to represent the experimental data.

$$P = a_0 + a_1 d + a_2 d^2 \qquad (3)$$

where a_0, a_1 and a_2 are constants. P is load in N and d is the indentation diagonal length in mm. a_0 and a_1 are function of true hardness, surface energy and experimental errors and the value of a_2 depends only on the true hardness given by

$$a_2 = H_T/1.8544 \qquad (4)$$

where H_T is the true microhardness of the test material, independent of indenter geometry and indentation size. Also from Equation 3

$$\Delta H = H_v - H_T = 1.8544\left(\frac{a_0}{d^2} + \frac{a_1}{d}\right) \qquad (5)$$

where H_v is the apparent Vickers hardness number expressed in GPa, H_T is the true hardness and ΔH is the difference between apparent hardness and true hardness. In the case of reverse indentation size effect (RISE) in which apparent hardness increases with increasing indentation size ΔH increases with increase in d.

3. Results

Variation of microhardness of the glass samples with applied load is shown in Fig. 1. All the 20 glass samples in the present study showed similar variations. It can be seen that (Fig. 1) the hardness number increases rapidly at lower values of the load, then increase at a slower rate and finally attains practically a constant value.

Typical plots of indentation diagonal length (d) vs. applied load (P) for selected glass samples under study are shown in Fig. 2. The solid lines in the plots are obtained by polynomial regression according to Equation 3. From the figure it is clear that Equation 3 can be used to represent the experimental data. The best-fit parameters included in the Equation 3 for all the 20 samples are recorded in Tables I and II. The true hardness value H_T is calculated from Equation 4.

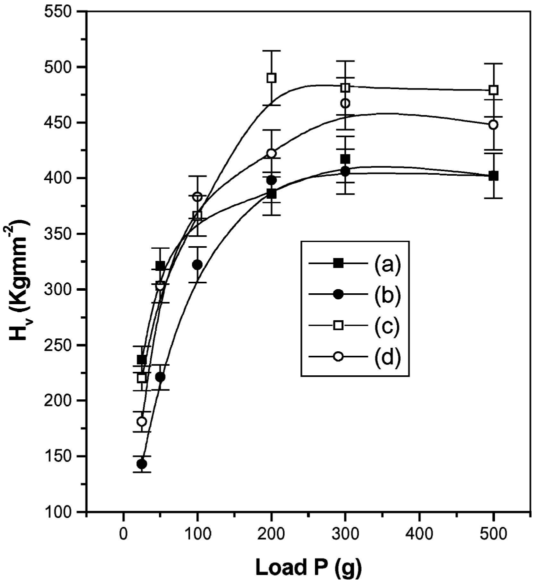

Figure 1 Variation of microhardness (H_v) with load (P) of (a) $60B_2O_3$-$30PbO$-$10PbCl_2$, (b) $50B_2O_3$-$40PbO$-$10PbCl_2$, (c) $60B_2O_3$-$30PbO$-$10CdCl_2$, and (d) $50B_2O_3$-$40PbO$-$10CdCl_2$ glasses.

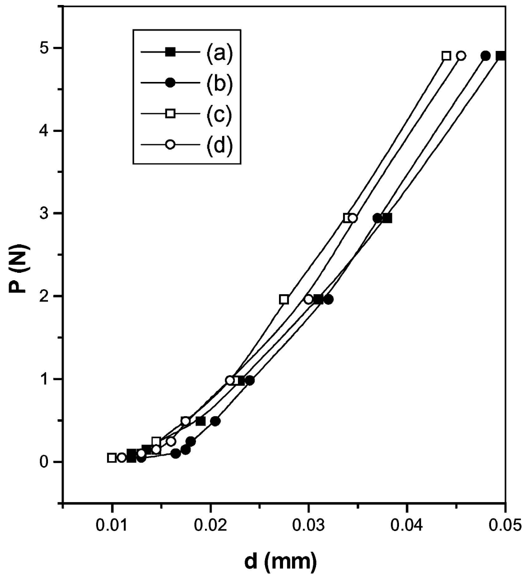

Figure 2 Plot of indentation size (d) as a function of applied load (P) for (a) $60B_2O_3$-$30PbO$-$10PbCl_2$, (b) $50B_2O_3$-$40PbO$-$10PbCl_2$, (c) $60B_2O_3$-$30PbO$-$10CdCl_2$, and (d) $50B_2O_3$-$40PbO$-$10CdCl_2$ glasses.

Plots of true microhardness number (H_T) vs. mole percentage of $PbCl_2$ or $CdCl_2$ contained in the glass samples are shown in Fig. 4. It can be seen that the true microhardness value (H_T) decreases with increase in mole percentage of $PbCl_2$ or $CdCl_2$ (Fig. 4).

4. Discussions

4.1. Indentation size effect

In Vickers hardness tester, the diamond indenter is a square pyramid and the shape of the indentation does not vary with load. According to the principle of geometrical similarity, a large indentation is a magnified picture of a small indentation. Hence hardness should be independent of the load [1]. But, experimentally measured microhardness number in the low load region decreases (ISE) or increases (RISE) with increase in load. In the present study it can be seen from Fig. 1 that in the low load region measured microhardness increases with increase in load. This indentation load or size effect on the microhardness, was attributed to a verity of phenomenon like work hardening during indentation [2], load to initiate plastic deformation [11], the indentation elastic recovery [15], plastic deformation band spacing [16] and effect of distorted zone [6, 7] etc. Surface polishing of the sample prior to indentation can also be a cause of ISE, because surface polishing introduces plastic deformation and cracks into the material adjacent to the surface [12, 17]. But the exact cause of the indentation load or size effect has not satisfactorily been determined [5]. At small loads, the indenter may penetrate only to the vicinity of the surface. With increase in load, penetration depth increases. Beyond a certain limit, the indenter penetrates beyond the surface and the bulk density of inner zone may be different from the surface density. For all the glass samples in the present study [$60B_2O_3$-$(40-x)PbO$-$xPbCl_2$, $60B_2O_3$-$(40-x)PbO$-$xCdCl_2$, $50B_2O_3$-$(50-x)PbO$-$xPbCl_2$ and $50B_2O_3$-$(50-x)PbO$-$xCdCl_2$], H_v was found to be practically independent of the load above 100 g. Hennicke and Vaupel [18] reported that for silica glass samples the hardness was load independent above a critical load but load dependent below that load and the critical load was approximately 0.8 N for silica glasses [18].

Using the best-fit values of the parameters a_0 and a_1 listed in Tables I and II, the difference between the values of the apparent hardness and true hardness $\Delta H = H_v - H_T$ can be calculated as a function of indentation size according to Equation 5. Fig. 3 shows the typical plots of the absolute value of ΔH as a function of indentation size. It can be seen that ΔH decreases with increase in indentation size and hence with applied load. Beyond a limiting load, ΔH approaches zero.

The value of the true microhardness H_T, and experimentally determined microhardness H_v for an applied load of 200 g, for all the glass samples in the present study are given in Tables I and II. It was found that value of H_v was larger than H_T in all most all cases (Tables I and II). The test specimens used in the present study were polished mechanically. Surface polishing removes material mechanically and introduces residual stresses on the surfaces of test specimen [19, 20] which in turn produces plastic deformation and cracks in the region adjacent to the surface [12, 13]. In the microhardness study of chalcogenides glasses of the system Se-Ge-As, Michels and Frischat [17] reported that some of glass samples showed a difference in surface hardness and volume hardness and it was attributed to the influence of surface polishing. In microhardness testing, a sharp indenter plastically deforms small volume of the material adjacent to the surface. Although a qualitative analysis relating to the effect of plastically deformed surface on the hardness is still lacking [12], there are reasons to believe that the experimentally observed microhardness values (H_v) are different from the true microhardness value (H_T) (Tables I and II). The true microhardness value (H_T) is independent of the indentation size and is free from the possible experimental errors in microhardness testing.

4.2. Compositional dependence

The dependence of Vickers microhardness number H_v on the composition is presented in Fig. 4 can be explained on the basis of structural changes occurring in the borate glass matrix. The change from triangular BO_3 to tetrahedral BO_4 groups with decreasing mole percentage of B_2O_3 is the major feature of the structural change in binary [21] and ternary borate glasses [22]. In addition, the non-bridging oxygen (NBO) in borate glasses plays an important role in deciding the structural changes with composition of glasses. The presence of BO_4 tetrahedra with bridging oxygen in the glass structure will cause maximum connectivity of the

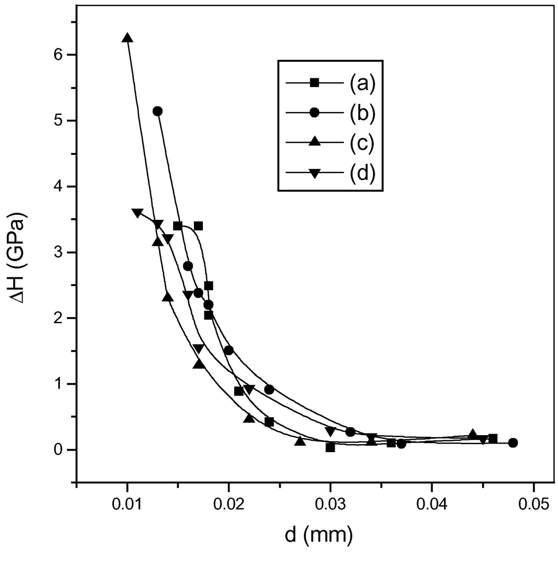

Figure 3 Plot of absolute value of ΔH as a function of indentation size for (a) $60B_2O_3$-30PbO-$10PbCl_2$, (b) $50B_2O_3$-40PbO-$10PbCl_2$, (c) $60B_2O_3$-30PbO-$10CdCl_2$, and (d) $50B_2O_3$-40PbO-$10CdCl_2$ glasses.

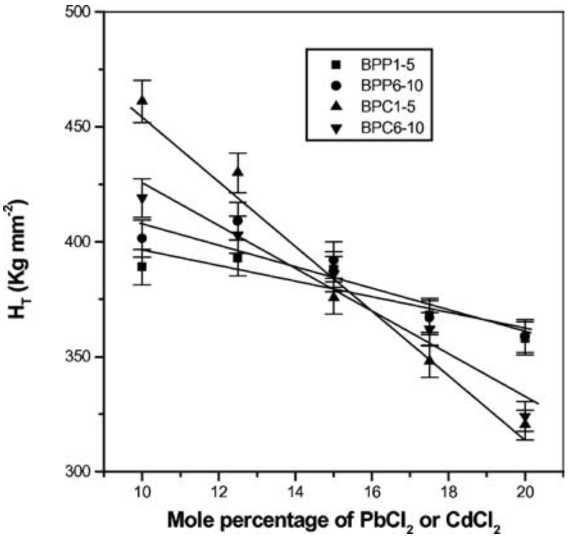

Figure 4 Plot of true microhardness number H_T vs. mole percentage of $PbCl_2$ or $CdCl_2$ in $60B_2O_3$-$(40-x)PbO$-$xMCl_2$ and $50B_2O_3$-$(50-x)PbO$-$xMCl_2$ (M = Pb, Cd) glasses.

glass network giving more rigidity to the structure and resulting in an increase in microhardness.

Doweidar *et al.* [23] reported the study of microhardness of ZnO-PbO-B_2O_3 glasses and observed that a sudden decrease of microhardness (H_v) number occurred between 60 and 62.5 mole percentage of (ZnO + PbO). The decrease in microhardness was attributed to the expansion of glass network due to the formation of non-bridging oxygen.

It is generally accepted that the molecular building block of vitreous B_2O_3 is planar BO_3 triangles, which are linked at the corners to form two-dimensional network [24]. The addition of PbO to the B_2O_3 network converts BO_3 units into BO_4 tetrahedra until one half of the boron-oxygen units are tetrahedra, with Pb^{2+} ions acting as charge compensators for negatively charged BO_4^- units [25–27]. Beyond this concentration, the structure begins to depolymerized and non-bridging oxygens (NBO) are formed in the network.

For a constant concentration of B_2O_3, when $PbCl_2$ is substituted for PbO in B_2O_3-PbO-$PbCl_2$ glass system, a local change in the structure is expected [28]. Substitution of $PbCl_2$ for PbO results in direct replacement of one O^{2-} ion for two Cl^- ions. As more and more $PbCl_2$ is substituted for PbO, the Cl^- ion concentration in the network increases. In addition, the ionic radius of Cl^- ions (0.181 nm) is larger than that of O^- ions (0.132 nm). As a result the glass network becomes systematically weakened and a more open network is formed, in order to accommodate of the excess chlorine ions [28]. Development of an open structure through the formation of non-bridging chlorine [26] or non-bridging oxygen would, there for lower the microhardness of the glass samples in the present study.

In order to check whether decrease in microhardness value was due to the excess Cl^- ions in the network, in the case of $60B_2O_3$-(40-x)PbO-$x$$CdCl_2$, $50B_2O_3$-(50-x)PbO-$x$$CdCl_2$ glasses, $CdCl_2$ was substituted for PbO, in a similar fashion as $PbCl_2$ was substituted for PbO in $60B_2O_3$-(40-x)PbO-$x$$PbCl_2$ and $50B_2O_3$-(50-x)PbO-$x$$PbCl_2$ glasses. In $60B_2O_3$-(40-x)PbO-$x$$PbCl_2$ and $50B_2O_3$-(50-x)PbO-$x$$PbCl_2$ glasses when $PbCl_2$ was substituted for PbO, the total Pb content remained constant in the glass system while the chlorine ion concentration increased. But in $60B_2O_3$-(40-x)PbO-$x$$CdCl_2$, $50B_2O_3$-(50-x) PbO-$x$$CdCl_2$ glasses, $CdCl_2$ was substituted for PbO, the chlorine ion concentration increased in a similar way as in the case of $60B_2O_3$-(40-x)PbO-$x$$PbCl_2$ and $50B_2O_3$-(50-x) PbO-$x$$PbCl_2$ glasses, while the Pb content concentration decreased. The variation of true hardness value (H_T) in $CdCl_2$ substituted glasses show a variation similar to that of $PbCl_2$ substituted glasses (Fig. 4) indicating that decrease in microhardness value is due to the expansion of network due to the excess of Cl^- ions in the network and not due to the cations (Pb^{2+}, Cd^{2+}) in the glass structure.

5. Conclusion

Vickers microhardness of glasses of the system $60B_2O_3$-(40-x) PbO-$x$$MCl_2$ and $50B_2O_3$-(50-x)PbO-$x$$MCl_2$ (M = Cd, Pb) was investigated for 20 different glass compositions. The hardness number showed an increase in its value up to a load of 200 g and then became practically a constant. At smaller loads (<100 g), the hardness increased rapidly. The indentation size effect (ISE) on the microhardness was discussed and the load independent true microhardness values were evaluated. The decrease of true microhardness with increase in mole percentage of $PbCl_2$ or $CdCl_2$was discussed on the basis of expansion of the glass network due to the incorporation of excess of Cl^- ions in the network.

Acknowledgments

One of the authors Shajo Sebastian acknowledges the University Grants Commission, Govt. of India, for financial support.

References

1. W. MASON, P. F. JOHNSON and J. R. VARNER, *J. Mater. Sci.* **26** (1991) 6576.
2. B. W. MOTT, in "Micro-indentation Hardness Testing" (Butterworths Scientific Publication, London, 1956).
3. G. N. BABINI, A. BESSOSI and C. GALASSI, *J. Mater. Sci.* **22** (1987) 1687.
4. K. HIRAO, M. TOMOZAWA, *J. Amer. Ceram. Soc.* **70** (1987) 497.
5. H. LI and R. C. BRADT, *J. Mater. Sci.* **28** (1993) 917.
6. M. S. JOSHI, V. V. JOSHI, A. L. CHOUDHARI and R. C. KANITHKAR, *ibid.* **19** (1984) 337.
7. C. C. DESAI and M. S. W. RAMANA, *ibid.* **23** (1988) 617.
8. P. FALTHAM and R BANERJEE, *ibid.* **27** (1992) 1626.
9. J. H. GONG and Y. LI, *ibid.* **35** (2000) 209.
10. E. MAYER, *Phys. Z* **9** (1908) 66.
11. C. HAYS and E. G. KENDALL, *Metall.* **6** (1973) 275.
12. J. H. GONG, J. J. WU and Z. D. GUAN, *Mater. Lett.* **35** (1998) 58.
13. *Idem., J. Matter. Sci. Lett.* **17** (1998) 473.
14. F. FROHLICH, P. GRAU and W. GRELLMANN, *Phys. Status Solidi* **42** (1977) 79.
15. D. R. TATE, *Trans. ASM* **35** (1945) 374.
16. S. J. BULL, T. F. PAGE and E. H. YOFFE, *Phil. Mag. Lett.* **59** (1989) 281.
17. B. D. MICHELS and G. H. FRISCHAT, *J. Mater. Sci.* **17** (1982) 329.
18. H. W. HANNICKLE and H. VAUPEL, *Glasstech. Ber* **49** (1976) 135.
19. R. SAMUEL, S. CHANDRASEKAR, T. N. FARRIS and R. H. LICHT, *J. Am. Ceram. Soc.***72** (1989) 1960.
20. F. F. LANGE, M. R. JAMES and D. J. GREEN, *ibid.* **66** (1983) C-16.
21. S. GREENBLATT and P. J. BRAY, *ibid.* **8**(6) (1967) 213.
22. W. L. KONIJNEND, *ibid.* **17**(6) (1976) 205.
23. H. DOWEIDAR, G. EL-DAMRAWI, Y. M. MOUSTAFA and A. K. HASSAN, *Phys. Chem. Glasses* **40** (1999) 252.
24. D. L. GRISCOM, in "Borate Glasses: Structure, Properties and Applications," edited by L. D. Pye, V. D. Frechette and N. J. Kreidl (Plenum, New York, 1978).
25. P. J. BRAY, M. LEVENTHAL and H. O. HOOPER, *Phys. Chem. Glasses* **4** (1963) 47.
26. C. A. GRESSLER and J. E. SHELBY, *J. Appl. Phys.* **66** (1989) 1127.
27. H. DEWEIDAR, I. A. GOHAR, A. MEGHED and G. EL-DAMRAWI, *Solid State Ion.* **46** (1991) 275.
28. G. EL-DAMRAWI, *J. Non. Cryst. Solids* **176** (1994) 91.

Received 19 January
and accepted 14 October 2004